



**HAL**  
open science

# Derivatization of the Peptidic Xxx-Zzz-His Motif toward a Ligand with Attomolar Cu II Affinity under Maintaining High Selectivity and Fast Redox Silencing

Katharina Zimmerer, Bertrand Vilenon, Carlos Platas-Iglesias, Bharath Vinjamuri, Angélique Sour, Peter Faller

## ► To cite this version:

Katharina Zimmerer, Bertrand Vilenon, Carlos Platas-Iglesias, Bharath Vinjamuri, Angélique Sour, et al.. Derivatization of the Peptidic Xxx-Zzz-His Motif toward a Ligand with Attomolar Cu II Affinity under Maintaining High Selectivity and Fast Redox Silencing. *Inorganic Chemistry*, 2023, 62 (24), pp.9429-9439. 10.1021/acs.inorgchem.3c00480 . hal-04182665

**HAL Id: hal-04182665**

**<https://hal.science/hal-04182665>**

Submitted on 17 Aug 2023

**HAL** is a multi-disciplinary open access archive for the deposit and dissemination of scientific research documents, whether they are published or not. The documents may come from teaching and research institutions in France or abroad, or from public or private research centers.

L'archive ouverte pluridisciplinaire **HAL**, est destinée au dépôt et à la diffusion de documents scientifiques de niveau recherche, publiés ou non, émanant des établissements d'enseignement et de recherche français ou étrangers, des laboratoires publics ou privés.

## Derivatization of the peptidic Xxx-Zzz-His motif towards a ligand with atto-molar Cu<sup>II</sup>-affinity under maintaining high selectivity and fast redox silencing

Katharina Zimmerer<sup>a</sup>, Bertrand Vileno<sup>a</sup>, Carlos Platas-Iglesias<sup>b</sup>, Bharath Vinjamuri<sup>a</sup>, Angélique Sour<sup>a\*</sup>, Peter Faller<sup>a,c\*</sup>

<sup>a</sup>Institut de Chimie (UMR 7177), Université de Strasbourg – CNRS, 4 Rue Blaise Pascal, 67000 Strasbourg, France.

<sup>b</sup> Departamento de Química Fundamental, Universidade da Coruña, Campus da Zapateira, Rúa da Fraga 10, 15008 A Coruña, Spain.

<sup>c</sup> Institut Universitaire de France (IUF), 1 rue Descartes, 75231 Paris, France.

### Abstract

Cu-chelation in biological systems is of interest as a tool to study the metabolism of this essential metal or for applications in case of diseases with a systemic or local Cu-overload, such as Wilson's or Alzheimer's disease. The choice of the chelating agent must meet several criteria. Among others, affinities and kinetics of metal-binding, and related metal-selectivity are important parameters of the chelators to consider. Here, we report on the synthesis and characterization of Cu-binding properties of two ligands, L1 and L2, derivatives of the well-known peptidic Cu<sup>II</sup>-binding motif Xxx-Zzz-His (also called ATCUN), where Cu<sup>II</sup> is bound to the N-terminal amine, two amidates and the imidazole. In either L, the N-terminal amine was replaced by a pyridine, and for L2, one amide was replaced by an amine compared to Xxx-Zzz-His. In particular, L2 showed several interesting features, including an affinity with a  $\log K_D^{\text{app}} = -16.0$  equals EDTA and higher than all reported ATCUN peptides. L2 showed high selectivity for Cu<sup>II</sup> over Zn<sup>II</sup> and other essential metal ions, even under the challenging conditions of the presence of human serum albumin. Further, L2 showed fast and efficient Cu<sup>II</sup> redox silencing qualities and stability in the presence of mM GSH concentrations. Including the fact that L2 can be easily elongated on its peptide part by standard SPPS to add other functions, L2 has attractive properties as a Cu<sup>II</sup> chelator for application in biological systems.

### Introduction

Copper (Cu) ions play an important role in several biological processes for most of the living beings. Cu in biology exists mainly in the two oxidation states Cu<sup>I</sup> and Cu<sup>II</sup>. Cu<sup>I</sup> is the prevalent form intracellularly, often attributed to the presence of high concentrations of thiols, in particular glutathione (GSH).<sup>1,2</sup> GSH and the other thiols are able to reduce Cu<sup>II</sup> rapidly to Cu<sup>I</sup> and the coordination to cysteine thiolates stabilizes the Cu<sup>I</sup> over Cu<sup>II</sup> redox state.<sup>3</sup> In the more oxidizing extracellular environment, Cu<sup>II</sup> is more prevalent, in particular the more labile and accessible pool of Cu<sup>II</sup> is bound to human serum albumin (HSA).<sup>4,5</sup>

Cu metabolism is tightly controlled, as an excess or lack of Cu as well as misplaced Cu can be dangerous. Hence Cu<sup>I/II</sup> ions are almost exclusively bound to proteins with high affinities, and Cu-transfer reactions occur normally via an associative mechanism. Overload of Cu is harmful by leading to trans-metalation (like with iron (Fe) in iron-sulfur clusters), binding and/or reacting with essential cysteines, catalysis of reactive oxygen species (ROS) generation and induction of protein misfolding.<sup>6-11</sup> Notably, Cu ions can be very potent in catalyzing ROS production in presence of a reducing agent and dioxygen.<sup>12,13</sup> The catalytic activity depends on the coordination environment of the Cu ion, which controls the redox

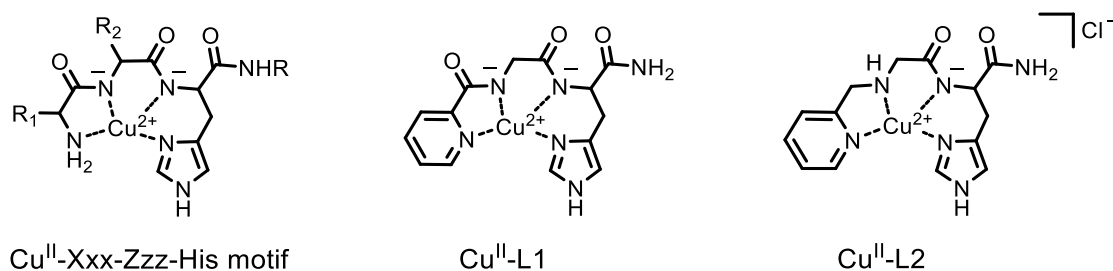
activity and reactivity.<sup>14–16</sup> Often, so-called loosely bound Cu or "free" Cu, such as Cu in a buffer or Cu bound in a less controlled and/or dynamic way to ligands are highly competent in ROS production.<sup>17</sup>

Some Cu-complex examples that attracted recent interest are composed of Cu bound to intrinsically disordered proteins, which are often also amyloidogenic. Intensively studied systems are Cu-complexes with amyloid-beta (A $\beta$ ), alpha synuclein and prion-protein, linked to Alzheimer's, Parkinson and prion diseases, respectively.<sup>18–21</sup>

There is a short peptide motif, consisting of the three N-terminal amino acids Xxx-Zzz-His, also called ATCUN (amino-terminal copper and nickel) motif. Xxx and Zzz can be any amino acid, apart from Pro for Zzz while a histidine (His) stands on the third position. This motif binds Cu<sup>II</sup> with a quite strong affinity (log  $K_D$  at pH 7.4 from -12.4 to -14.7).<sup>22–25</sup> Moreover, the motif shows a high selectivity for Cu<sup>II</sup> over other relevant essential metal ions (Zn<sup>II</sup>, Fe<sup>III</sup>, Mn<sup>II</sup>, Ca<sup>II</sup> and Mg<sup>II</sup>), mainly attributed to the higher stability of the Cu<sup>II</sup> complex that is able to deprotonate the two amide protons to bind the amidates at around neutral pH. Another interesting feature is, that Xxx-Zzz-His binds Cu<sup>II</sup> with a rigid square planar coordination by two amines and two amidates, including two 5 and one 6-membered ring (see Scheme 1). This highly Cu<sup>II</sup>-stabilizing coordination is associated to a low redox potential that inhibits redox-cycling between Cu<sup>II</sup> and Cu<sup>I</sup> and hence restrains the catalysis of ROS production almost completely.<sup>26–31</sup> A residual activity has been recently assigned to a very low populated Cu<sup>II</sup> coordination to Xxx-Zzz-His without amidate coordination.<sup>32</sup> The ATCUN motif is the native Cu<sup>II</sup>-binding site of serum albumin (with the sequence Asp-Ala-His in HSA) and has been more recently employed for its ability to suppress ROS production.<sup>23,33–36</sup> Indeed, peptides with Xxx-Zzz-His motifs are able to withdraw Cu<sup>II</sup> from A $\beta$ <sub>1-16/40/42</sub> peptides (and others) and can suppress Cu-A $\beta$  catalyzed ROS production in presence of ascorbate and dioxygen.<sup>34,37–41</sup> Moreover, a truncated form of A $\beta$  (A $\beta$ <sub>4-x</sub>) contains also this motif and can retrieve Cu<sup>II</sup> from A $\beta$ <sub>1-x</sub> and hence redox silence the Cu<sup>II</sup>.<sup>42</sup>

In the present work, we explore the possibility to modify this Xxx-Zzz-His motif in terms of higher affinities and by keeping the Cu<sup>II</sup>-selectivity, still based on peptide chemistry. Hence, we designed two new ligands, L1 and L2 (Scheme 1).

**Scheme 1. Representation of the Cu<sup>II</sup>-complexes with the Xxx-Zzz-His/ATCUN motif and the ligands L1 and L2.**



## Results and Discussion

### Design and synthesis of the ligands.

The two tetradentate ligands L (with L = L1, L2) were designed based on the well-known Cu<sup>II</sup>-binding ATCUN motif. In L1 and L2, the N-terminal amine is replaced by a pyridine. Pyridine has normally a stronger affinity compared to an amine at neutral pH, hence an increase in affinity of L1 and L2 compared to the simplest motif (Gly-Gly-His) is expected. In addition, for L2 one of the two amide functions (between Xxx and Zzz) is replaced by an amine, again with the idea to increase the affinity by replacing an amidate with an amine, but with the risk of losing selectivity towards Cu<sup>II</sup>.

Both ligands were synthesized by standard solid-phase peptide synthesis (SPPS) procedure. The C-terminal position is of importance, as it would be straightforward to elongate the peptide on the C-terminal end. Hence, either L could be elongated with a peptide to add another function, as peptides are versatile platforms. The synthesis was performed on a Rink Amide resin starting with the attachment of His(Trt) and Gly. Then, 2-picolinic acid was used for the introduction of the pyridinyl derivative in the last coupling step to obtain L1. For L2 a nucleophilic substitution reaction involving 2-picolyl chloride hydrochloride constitutes the last synthetic step. After cleavage from the resin and removal of the protecting groups, the ligands L were purified by HPLC and characterized by 1D and 2D NMR and HR-ESI-MS (see SI section 1).

### Characterization of the Cu<sup>II</sup>-L complexes by electronic absorption and EPR.

The Cu<sup>II</sup>-binding stoichiometry and spectroscopic characteristics were investigated. L1 and L2 were titrated by Cu<sup>II</sup> in HEPES buffer at pH 7.4 and the formed complexes were characterized by UV-Vis (Figure S15). For L1 and L2, characteristic d-d bands were evolving in a regular manner up to one equivalent, and then leveled off. This is in line with the formation of a stoichiometric 1:1 complex for L1 and L2 with Cu<sup>II</sup>. The d-d absorption bands were centered at  $\lambda_{\max} = 552$  nm and 564 nm for Cu<sup>II</sup>-L1 and Cu<sup>II</sup>-L2, respectively. The molar extinction coefficient  $\epsilon$  had typical values for d-d bands of 116 M<sup>-1</sup>cm<sup>-1</sup> for Cu<sup>II</sup>-L1 and 97 M<sup>-1</sup>cm<sup>-1</sup> for Cu<sup>II</sup>-L2. The red shift of the band of Cu<sup>II</sup>-L2 compared to Cu<sup>II</sup>-L1 is in line with the lower ligand field generated by a neutral amine against a negatively charged amidate. Indeed, according to a formula<sup>1</sup> reported in the literature, Cu<sup>II</sup>-L1 is predicted to have the  $\lambda_{\max}$  at 537 nm whereas Cu<sup>II</sup>-L2 at 547 nm (by treating the pyridine like an imidazole).<sup>43</sup> These calculated values are slightly too blue shifted, which might be partially due to our approximation of equivalent contribution of pyridine and imidazole.

To further characterize the Cu<sup>II</sup>-L complexes, low temperature EPR was employed. Both Cu<sup>II</sup>-L complexes showed typical EPR spectra for square planar Cu<sup>II</sup>-coordination (Figure 1, Figure S16 and Table 1). The higher  $g_{\parallel}$  value for Cu<sup>II</sup>-L2 ( $g_{\parallel} = 2.205$ ) than Cu<sup>II</sup>-L1 ( $g_{\parallel} = 2.194$ ) are in line with the absorption spectra and the higher ligand field in Cu<sup>II</sup>-L1. The superhyperfine interactions in the  $g_{\perp}$  region are consistent with the coupling to four nitrogens.

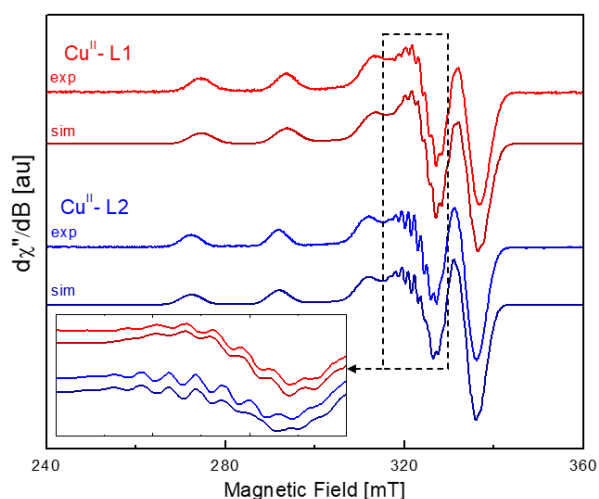


**Figure 1.** EPR experimental and simulated spectra of Cu<sup>II</sup>-L1 and Cu<sup>II</sup>-L2 (600  $\mu$ M L, 500  $\mu$ M CuCl<sub>2</sub>, 50 mM HEPES buffer pH 7.4, supplemented by 10% glycerol v/v, at 100 K).

<sup>1</sup>  $\lambda_{\max} = 1000/[1.18 + 0.140(lm) + 0.166(NH_2) + 0.200(N = (\text{amidate}))]$

In summary visible and EPR spectroscopies suggest that Cu<sup>II</sup> forms a well-defined 1:1 complex with L1 and L2 according to the initial design (see Scheme 1).

The structures of the Cu<sup>II</sup>-L1 and Cu<sup>II</sup>-L2 complexes were also investigated using density functional theory (DFT) calculations. The optimized geometries of the two complexes display the expected square planar coordination around Cu<sup>II</sup> (Figure 2). The Cu<sup>II</sup>-N bond distances in Cu<sup>II</sup>-L1 are very similar to those observed by X-ray diffraction for the complex with Gly-Gly-His-N-methyl amide.<sup>44</sup> The substitution of a negatively charged amidate donor in Cu<sup>II</sup>-L1 by an amine in Cu<sup>II</sup>-L2 results in a significant elongation of the corresponding Cu-N bond, as would be expected. The square-planar coordination environment is more distorted in Cu<sup>II</sup>-L2 than in Cu<sup>II</sup>-L1, as judged by the mean deviation of the N donor atoms from the least-squares plane defined by the CuN4 core (0.128 and 0.270 Å, respectively). This is in line with the lower crystal field generated by the ligand in Cu<sup>II</sup>-L2 compared with Cu<sup>II</sup>-L1.

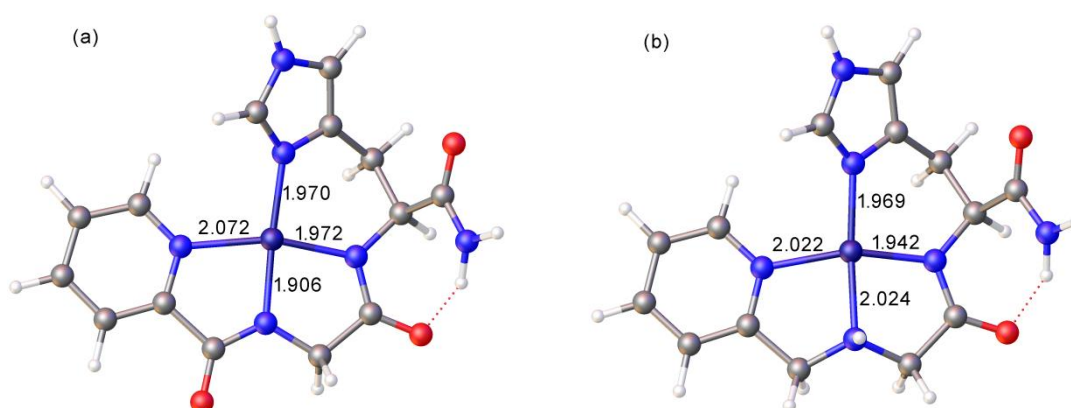


**Figure 2.** Structures of the Cu<sup>II</sup>-L1 (a) and Cu<sup>II</sup>-L2 (b) complexes obtained with DFT calculations (uwB97XD/Def2tzvp). Numbers correspond to the calculated bond distances of the Cu<sup>II</sup> coordination sphere (Å).

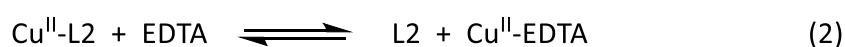
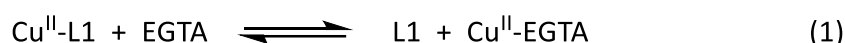
The quality of the DFT structures was assessed by comparison of the experimental and calculated EPR parameters (Table 1). The *A*-tensors were computed at the TPSSh/Def2-QZVPP level, as the hybrid meta-GGA functional was found to provide accurate hyperfine coupling constants for both organic radicals and metal complexes, including Cu<sup>II</sup> complexes.<sup>45,46</sup> The *g*-tensors were calculated using the double-hybrid density functional PBE0-DH, following a recently described methodology.<sup>47</sup> The calculated EPR parameters are in very good agreement with the experiment. This is especially the case for the hyperfine coupling constants. Both approaches characterize Cu<sup>II</sup>-L1 with slightly lower *g*<sub>||</sub> and *A*<sub>||</sub> values than Cu<sup>II</sup>-L2, while the trend in <sup>14</sup>N *A*<sub>iso</sub> values is reversed.

**Table 1.** Parameters obtained from the fits of EPR<sup>a</sup> spectra and obtained with DFT calculations.

		<i>g</i> <sub>  </sub>	<i>g</i> <sub>⊥</sub>	<i>A</i> <sub>  </sub> / MHz	<i>A</i> <sub>⊥</sub> / MHz	<sup>14</sup> N <i>A</i> <sub>iso</sub> / MHz <sup>b</sup>
Cu <sup>II</sup> -L1	Exp.	2.194	2.043	576	45 <sup>d</sup>	42
	DFT	2.175	2.049	580 <sup>c</sup>	37	41.4
Cu <sup>II</sup> -L2	Exp.	2.205	2.046	592	65 <sup>d</sup>	39
	DFT	2.192	2.053	592 <sup>c</sup>	14	35.9

<sup>a</sup>*g* and *A* strain parameters were used to account for experimental line broadening <sup>b</sup> Calculated values are averages over the *A*<sub>iso</sub> values obtained for the four N donor atoms. <sup>c</sup> Calculated as negative values. <sup>d</sup>*A*<sub>⊥</sub> is given on an indicative basis as being mostly unresolved experimentally.

**Cu<sup>II</sup> affinity of L1 and L2.** The binding affinity at pH 7.4 towards Cu<sup>II</sup> of L1 and L2 was investigated. Due to the high expected affinity, an indirect approach was employed by using well characterized competitors. Thus, only apparent relative affinities to the competitor can be obtained under the given condition (here 40 mM HEPES buffer whose pH has been adjusted to pH 7.4 with NaOH addition). Competition experiments were conducted with the well-characterized ligands EDTA (ethylene diamine tetraacetic acid) and EGTA (ethylene glycol-bis(2-aminoethyl ether)-tetraacetic acid). Cu<sup>II</sup>-EDTA and Cu<sup>II</sup>-EGTA have a dissociation constant at pH 7.4 ( $K_{D(pH7.4)}$ ) of  $10^{-15.9}$  and  $10^{-14.2}$  and exhibit d-d bands at 735 nm and 687 nm, respectively.<sup>48,49</sup> By assuming that the apparent  $K_{D(pH7.4)}$  in the here used buffer (named  $K_{D(pH7.4)}^{app}$ ) are similar to the calculated  $K_{D(pH7.4)}$ . Indeed, these competitors were very well suited as it turned out that their affinity is very similar to that of L1 and L2 and their d-d bands are rather well separated. This allows more accurate measurements. In order to make sure that the thermodynamic minimum of the chemical reactions 1 and 2:



was reached, the measurements were started from both sides, *i.e.* the competitor ligand (EDTA or EGTA) was added to Cu<sup>II</sup>-L, and ligand L was added to Cu<sup>II</sup>-EDTA or Cu<sup>II</sup>-EGTA (Figures 3 and 4). The kinetics were monitored and indeed, very similar end-point absorbances were reached (Figures 3C - 3D and 4C - 4D). As such the affinity at pH 7.4 was determined for L2 to be about 1.3 times stronger than EDTA, and for L1 about 4 times weaker than EGTA. By assuming that the  $K_{D(pH7.4)}^{app}$  values in the used buffer are similar to the calculated  $K_{D(pH7.4)}$  for EDTA and EGTA, we obtain  $K_{D(pH7.4)}^{app}$  values of  $10^{-13.6}$  for Cu<sup>II</sup>-L1 and  $10^{-16.0}$  for Cu<sup>II</sup>-L2 (see SI section 2.4). This would correspond to pCu<sup>app</sup> values of 14.6 for Cu<sup>II</sup>-L1 and 17.0 for Cu<sup>II</sup>-L2 (with 1  $\mu$ M Cu and 10  $\mu$ M L at pH 7.4).<sup>50</sup>

**Table 2: UV-Vis spectroscopic parameters and apparent stability constants and pCu values of Cu<sup>II</sup>-L1 and Cu<sup>II</sup>-L2.**

complex	$\lambda_{\text{max}}$ [nm]	$\epsilon$ [M <sup>-1</sup> ·cm <sup>-1</sup> ]	$K_{D(pH7.4)}^{app}$	pCu <sup>app</sup>
Cu <sup>II</sup> -L1	552	116	$10^{-13.6}$	14.6
Cu <sup>II</sup> -L2	564	97	$10^{-16.0}$	17.0

Hence, compared to Gly-Gly-His, the simplest ATCUN motif, replacing the amine by a pyridine led to an increase of  $K_{D(pH7.4)}$  by about one order of magnitude if one assumes  $K_{D(pH7.4)}^{app} = K_{D(pH7.4)}$ . (However, the determined  $\log K_{D(pH7.4)}$  of -12.2 or -12.4 are for Gly-Gly-His containing a COO<sup>-</sup> at the C-terminus position, not an amide like in L1, hence this could also contribute to the increase in the affinity of L1 compared to Gly-Gly-His.<sup>23,51</sup> The replacement of an amidate by an amine resulted in a higher affinity of about 1 to 2 log unit at pH 7.4, clearly above all the reported ATCUN motifs and at the same level as EDTA.

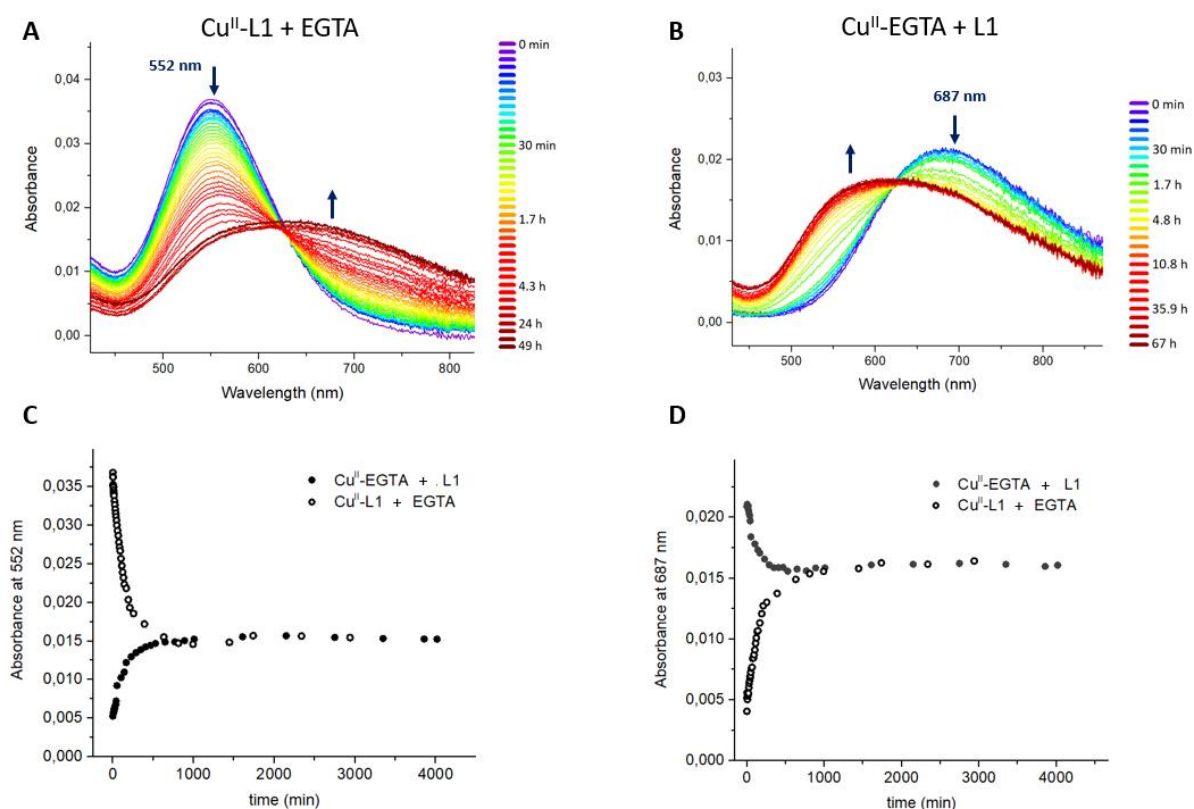


**Figure 3.** A and B: UV-Vis absorption spectra of the competition of A)  $\text{Cu}^{\text{II}}\text{-L1}$  with 1 eq. EGTA and B)  $\text{Cu}^{\text{II}}\text{-EGTA}$  with 1 eq. L1. The graphs C and D show the evolution of the absorption maximum of the d-d band of  $\text{Cu}^{\text{II}}\text{-L1}$  (C) and  $\text{Cu}^{\text{II}}\text{-EGTA}$  (D) over time. After approximately 800 min an equilibrium state is reached where the concentration of  $\text{Cu}^{\text{II}}\text{-L1}$  and  $\text{Cu}^{\text{II}}\text{-EGTA}$  are stable over time. Conditions: 400  $\mu\text{M}$  concentration of ligand and competitor, 320  $\mu\text{M}$   $\text{Cu}^{\text{II}}$  (0.8 eq.) in 40 mM HEPES buffer pH 7.4. The competition experiments were performed in triplicate and a representative experience is presented.

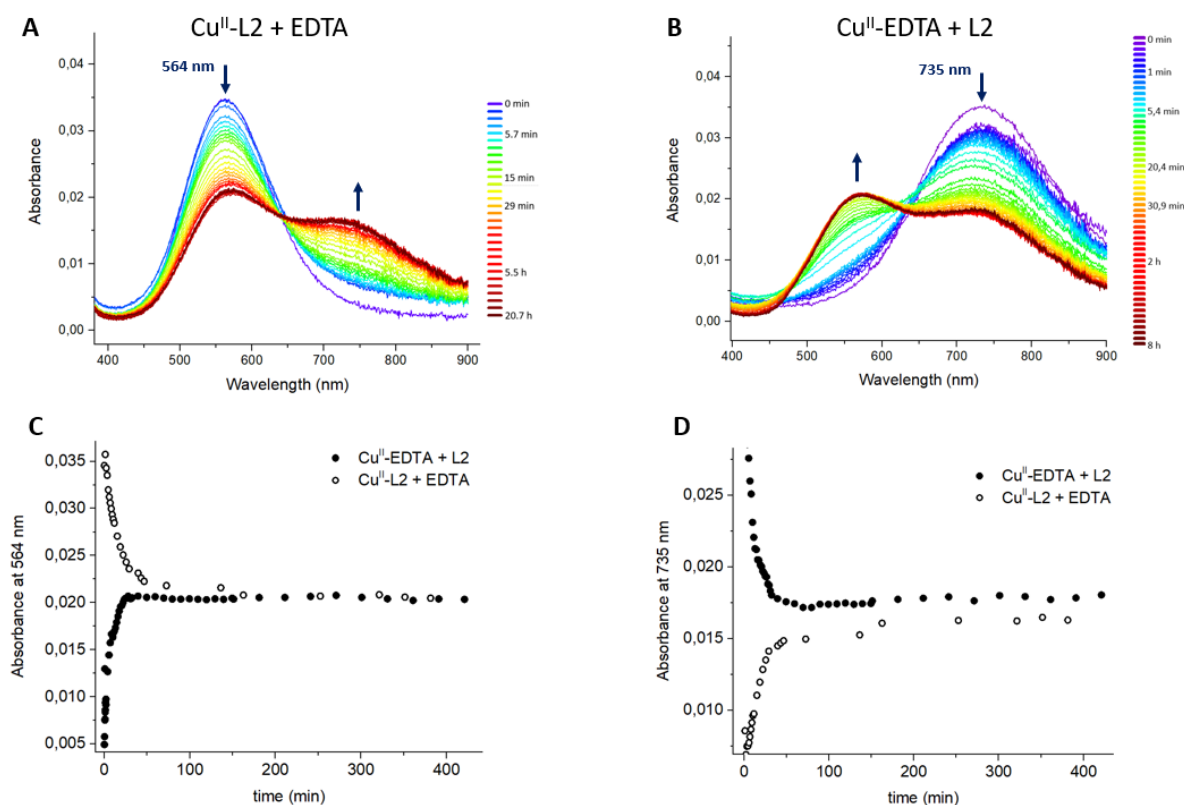


**Figure 4.** A and B: UV-Vis absorption spectra of the competition of A)  $\text{Cu}^{\text{II}}\text{-L2}$  with 1 eq. EDTA and B)  $\text{Cu}^{\text{II}}\text{-EDTA}$  with 1 eq. L1. The graphs C and D show the evolution of the absorption maximum of the d-d band of  $\text{Cu}^{\text{II}}\text{-L2}$  (C) and  $\text{Cu}^{\text{II}}\text{-EDTA}$  (D) over time. After approximately 70 min an equilibrium state is reached where the concentration of  $\text{Cu}^{\text{II}}\text{-L2}$  and  $\text{Cu}^{\text{II}}\text{-EDTA}$  are stable over time. Conditions: 400  $\mu\text{M}$  concentration of ligand and competitor, 320  $\mu\text{M}$   $\text{Cu}^{\text{II}}$  (0.8 eq.) in 40 mM HEPES buffer pH 7.4. The competition experiments were performed in triplicate and a representative experience is presented.

The pH-dependence complex formation was followed *via* the presence of the d-d absorption bands around 552 and 564 nm for  $\text{Cu}^{\text{II}}\text{-L1}$  and  $\text{Cu}^{\text{II}}\text{-L2}$  respectively (see Figure S17). Formation of  $\text{Cu}^{\text{II}}\text{-L1}$  starts at pH 3 and is complete at around pH 5. Formation of  $\text{Cu}^{\text{II}}\text{-L2}$  occurs at more acidic pH, roughly from pH 2 to pH 4.5. The stability to lower pH of  $\text{Cu}^{\text{II}}\text{-L2}$  is in agreement with the higher affinity constant  $\log K_{D(\text{pH}7.4)}$  value.

**Competition with  $\text{Cu}^{\text{II}}\text{-HSA}$  with/without the presence of  $\text{Zn}^{\text{II}}$  with CD and UV-Vis absorption spectroscopy.** Extracellularly, where  $\text{Cu}^{\text{II}}$  and  $\text{Zn}^{\text{II}}$  mostly occur together,  $\text{Zn}^{\text{II}}$  is much more available for chelation than  $\text{Cu}^{\text{II}}$ , due to its higher concentration and lower affinity to the native proteins. In the blood plasma, the  $\text{Cu}^{\text{II}}$  accessible for chelators, called labile or exchangeable Cu pool (mainly bound to HSA) with a  $K_{D(\text{pH}7.4)}$  of  $10^{-13}$ .<sup>48,52</sup> Most  $\text{Zn}^{\text{II}}$  is exchangeable and bound as well to HSA with a  $K_{D(\text{pH}7.4)}$  of  $10^{-7}$ .<sup>53,54</sup> Exchangeable  $\text{Zn}^{\text{II}}$  in the blood is about 10 times more abundant than  $\text{Cu}^{\text{II}}$  and  $10^6$  times less strongly bound. In other words, to mimic this situation the selectivity of  $\text{Cu}^{\text{II}}$ -binding over  $\text{Zn}^{\text{II}}$  would have to be achieved with a  $10^7$  times higher  $\text{Zn}^{\text{II}}$  concentration. This seems not feasible as it would demand insoluble high  $\text{Zn}^{\text{II}}$  concentration based on the low intensity d-d bands of  $\text{Cu}^{\text{II}}$ . To measure the selectivity in a more challenging situation like it is expected to be in the blood, we performed competition experiments with HSA, first to show that the ligands L1 and L2 are able to retrieve  $\text{Cu}^{\text{II}}$  from HSA, and then when HSA was loaded with  $\text{Cu}^{\text{II}}$  and  $\text{Zn}^{\text{II}}$ , to see the selectivity. The competition experiments were followed by UV-Vis absorption spectroscopy and circular dichroism (CD). The latter was used due to its better resolution of the d-d bands, and is in coherence with the data obtained by UV-Vis analyses (Figures S18-S21).



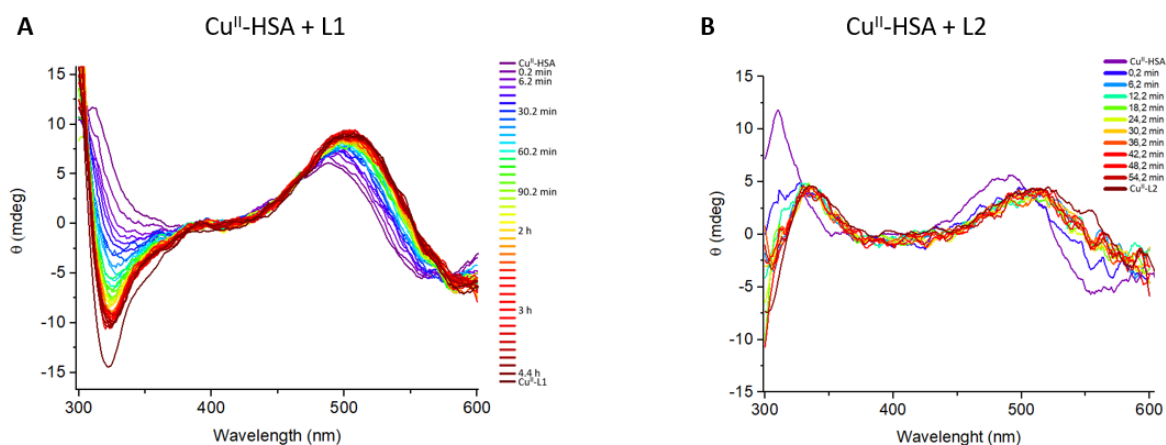


**Figure 5.** CD spectra of the competition experiment of Cu<sup>II</sup>-HSA with L1 (A) and L2 (B). Conditions: 500  $\mu$ M HSA, 450  $\mu$ M CuCl<sub>2</sub>, 50 mM, 500  $\mu$ M ligand, HEPES buffer pH 7.4. The endpoint of the competition was compared to the CD-spectrum of Cu<sup>II</sup>-L measured under the same conditions (500  $\mu$ M ligand, 450  $\mu$ M CuCl<sub>2</sub>, 50 mM HEPES pH 7.4). The CD-spectra of the competition experiments in the presence of Zn<sup>II</sup> (Zn<sup>II</sup>-Cu<sup>II</sup>-HSA with L and Cu<sup>II</sup>-L with Zn<sup>II</sup>-HSA) can be found in Figure S18.

Figure 5 shows the addition of L1 (left) and L2 (right) to Cu<sup>II</sup>-HSA (0.8:1). Cu<sup>II</sup>-HSA has a positive band at 320 nm and two bands in the region of the d-d bands, a positive at 490 nm and negative at 560 nm (as reported in the literature<sup>55</sup>). The addition of the ligand leads to an evolution of the spectra with a red shift for the d-d bands in either case. The reaction came to a halt after about 200 min for L1 and 20 min for L2, with a spectrum very similar to the Cu<sup>II</sup>-L alone. This is in line with the transfer of Cu<sup>II</sup> from HSA to the added ligand. To confirm that all Cu<sup>II</sup> was transferred to L, EPR spectra were collected at the end of the reaction (Figure S19 and Table S1). No signal for Cu<sup>II</sup>-HSA could be detected, indicating a transfer of Cu<sup>II</sup> close to completion, in line with the reported lower affinity of Cu for HSA ( $\log K_D = -13$ ).<sup>52</sup> L2 was about 10 times faster under the present condition to retrieve Cu<sup>II</sup> from HSA. This indicates that L2 is not only a stronger ligand than L1 and the ATCUN motif in general, but it is also quite fast in Cu<sup>II</sup> complexation.

The experiments were repeated in the presence of Zn<sup>II</sup>, *i.e.* L was added to Zn<sup>II</sup>-Cu<sup>II</sup>-HSA (0.8 : 0.8 : 1) and the reaction was followed by CD and verified at the end by EPR. The same endpoints were reached, meaning that the same amount of Cu<sup>II</sup> can be retrieved from HSA regardless of the presence of Zn<sup>II</sup> (Figure 6). This supports the high selectivity of L for Cu<sup>II</sup> over Zn<sup>II</sup> under this challenging condition. In the presence of Zn<sup>II</sup>, Cu<sup>II</sup> retrieval from HSA was slightly slower for L2, but not for L1 (Figure 6).

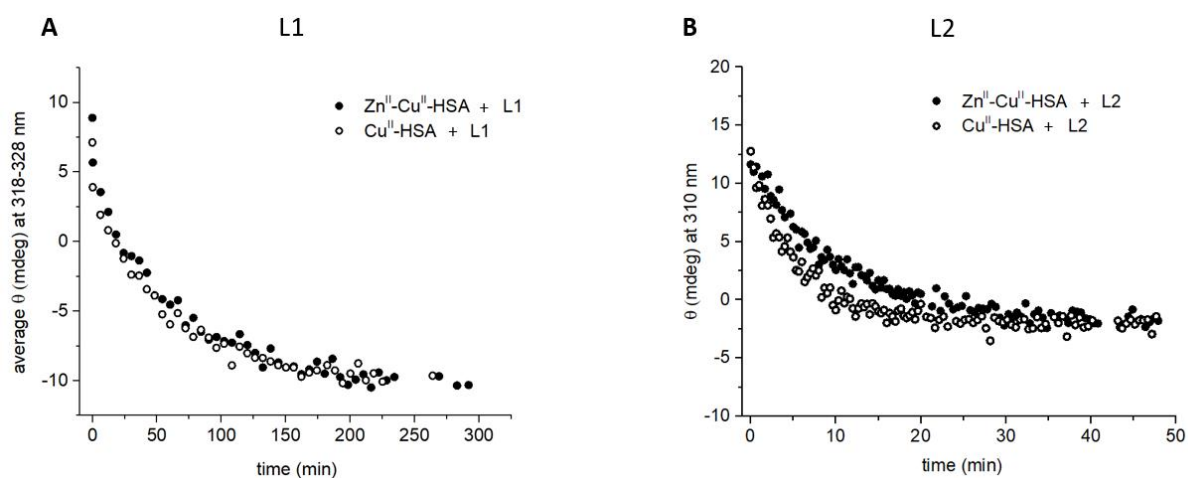


**Figure 6.** Comparison of the kinetics with and without the presence of Zn<sup>II</sup>. A) The evolution of  $\theta$  over time was monitored in the wavelength range of 300-600 nm by taking a spectrum every 6 min. As  $\theta$  of the start and end-point of the competition shows a huge difference in the wavelength region 318-328 nm, this averaged  $\theta$  value was used for the comparison of the competition with and without Zn<sup>II</sup>. B) As the kinetics of L2 is very fast, the evolution of  $\theta$  over time was monitored directly at

310 nm by doing a measurement every 20 s during the competition. Conditions: 500  $\mu\text{M}$  HSA, 450  $\mu\text{M}$   $\text{CuCl}_2$ , 450  $\mu\text{M}$   $\text{ZnSO}_4$ , 50 mM, 500  $\mu\text{M}$  ligand, HEPES buffer pH 7.4. The CD competition experiments were performed in duplicate for L1 and triplicate for L2 and representative experiments are presented.

**Selectivity over other metal ions.** Although less of an issue, the selective  $\text{Cu}^{\text{II}}$ -binding of L1 and L2 was also investigated in the presence of a mixture of essential metal ions ( $\text{Zn}^{\text{II}}$ ,  $\text{Fe}^{\text{III}}$ ,  $\text{Mn}^{\text{II}}$ ,  $\text{Ca}^{\text{II}}$  and  $\text{Mg}^{\text{II}}$ ) in the absence of HSA. These experiments were evaluated by UV-Vis absorption spectroscopy. The curves showed no decrease of the d-d band upon addition of a mixture of  $\text{Zn}^{\text{II}}$ ,  $\text{Fe}^{\text{III}}$ ,  $\text{Mn}^{\text{II}}$ ,  $\text{Ca}^{\text{II}}$  and  $\text{Mg}^{\text{II}}$ , indicating selectivity under these conditions (Figure S22). Moreover, up to 1000 eq. of  $\text{Zn}^{\text{II}}$  did not impact the d-d band intensity (Figure S23). This supports the high selectivity of L1 and L2 for  $\text{Cu}^{\text{II}}$ , as it is known for the parent Xxx-Zzz-His/ATCUN motif.<sup>23</sup>

**Redox-silencing.**  $\text{Cu}^{\text{II}}$ -complexes with ligands of the Xxx-Zzz-His/ATCUN type attracted quite a lot of interest in terms of ligands able to redox-silence  $\text{Cu}^{\text{II}}$ . In particular,  $\text{Cu}^{\text{II}}$  bound to amyloidogenic peptides, such as amyloid- $\beta$ , is supposed to be implicated in the development of Alzheimer's disease and to play a catalytic role in the production of ROS. In vitro, in the presence of ascorbate under aerobic conditions,  $\text{Cu-A}\beta_{1-16}$  is known to catalyze the oxidation of ascorbate with concomitant formation of ROS.<sup>56</sup> Therefore, the ability of the ligands L1 and L2 to redox silence  $\text{Cu-A}\beta_{1-16}$  were tested.

Figure 7 shows the ascorbate oxidation followed at 265 nm by absorption spectroscopy. Upon addition of  $\text{Cu}^{\text{II}}$ , the absorbance decreases due to the oxidation of ascorbate. The addition of L1 or L2 stops very rapidly and completely the ascorbate oxidation. No further oxidation occurs for the rest of the measured time (Figure 7A). In the case of the presence of  $\text{Cu}^{\text{II}}$  complexed to  $\text{A}\beta_{1-16}$  (Figure 7B), ascorbate oxidation started after the addition of  $\text{Cu-A}\beta_{1-16}$ . In line with the literature, the oxidation catalysis by the  $\text{Cu-A}\beta_{1-16}$  complex was slower compared to  $\text{Cu}^{\text{II}}$  in buffer.<sup>57,58</sup> Again, additions of L1 and L2 lead to an arrest of ascorbate oxidation. This occurred immediately in the case of L2, whereas for L1 ascorbate oxidation stopped completely only after about 10 min. This slower kinetic of L1 compared to L2 could be confirmed by experiments at 10 times lower concentrations of  $\text{Cu-A}\beta_{1-16}$  and L, which slowed down further the arrest of ascorbate oxidation by L1, in contrast to the still immediate arrest by L2 (Figure S24).

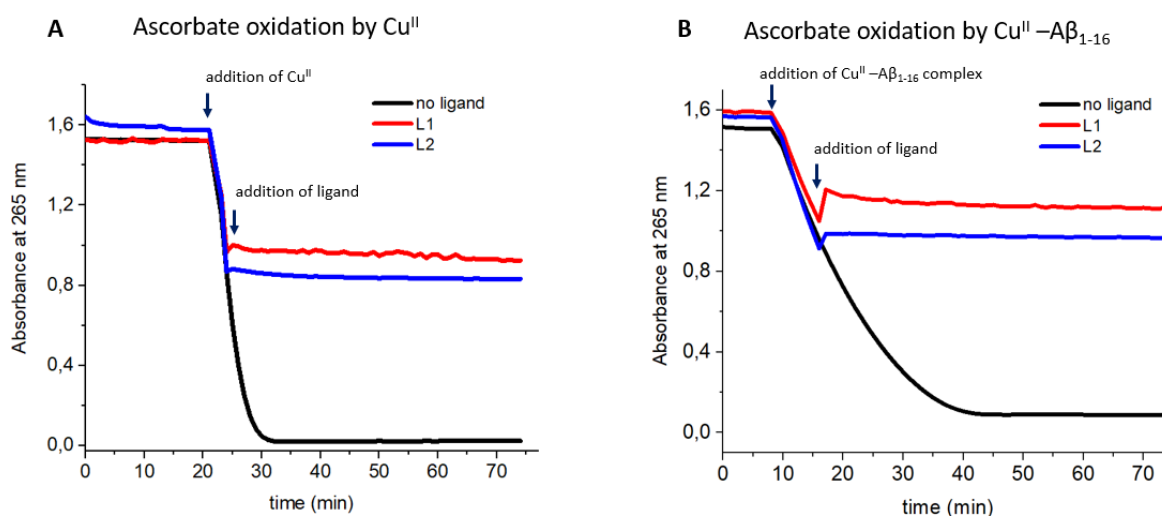


**Figure 7.** Evolution of the absorbance at 265 nm over time. Conditions: A) 100  $\mu\text{M}$  ascorbate, 10  $\mu\text{M}$   $\text{CuCl}_2$ , 20  $\mu\text{M}$  ligand, 50 mM HEPES buffer pH 7.4, B) 15  $\mu\text{M}$   $\text{A}\beta_{1-16}$  precomplexed with 10  $\mu\text{M}$   $\text{CuCl}_2$ , 30  $\mu\text{M}$  ligand, 100  $\mu\text{M}$  ascorbate, 50 mM HEPES buffer pH 7.4. Control experiments without the addition of any ligand are shown in black.

These experiments suggest that L1 and L2 efficient redox silencer, *i.e.* they form Cu<sup>II</sup>-complexes inert towards reduction by ascorbate. Moreover, L2 was able to retrieve Cu<sup>II</sup> rapidly from the Cu<sup>II</sup>-A $\beta$  complex, whereas L1 was more sluggish.

**Interaction of Cu<sup>II</sup>-L with GSH.** Another important reducing agent in biology is glutathione (GSH). GSH is present at mM concentrations (~1-10 mM) intracellularly, but only at low  $\mu$ M in the blood plasma.<sup>59</sup> GSH is not only a reducing agent, but also a strong chelator of Cu<sup>I</sup>.<sup>2</sup> Several Cu-Xxx-Zzz-His-peptide complexes have been investigated for their reaction with GSH. Classically, mM GSH concentrations were able to reduce Cu<sup>II</sup> and retrieve it from several ATCUN motifs to form Cu<sup>I</sup>-thiolate clusters, mainly Cu<sub>4</sub>-GSH<sub>6</sub>. This indicates that Cu-Xxx-Zzz-His/ATCUN complexes would be dissociated when entering the cell.<sup>60,61</sup> Also in the present case, 2 mM GSH was able to reduce Cu<sup>II</sup>-L1 under aerobic conditions slowly, with a  $t_{1/2}$  of about 120 min (Figure 8). However, it did not go to completion, as a plateau was reached. In contrast, no obvious reduction of the intensity of the d-d band was observed for Cu<sup>II</sup>-L2 over 20 hours, showing a remarkable inertness against reduction and withdrawal of Cu<sup>II</sup>-L2 by GSH.

Under anaerobic conditions, reduction of both Cu<sup>II</sup>-L1 and Cu<sup>II</sup>-L2 with GSH occurred (Figure 8 and Figure S25). This suggests that Cu<sup>II</sup>-L2 was only apparently stable under aerobic conditions, indeed GSH is able to reduce Cu<sup>II</sup> slowly and O<sub>2</sub> reoxidizes it more rapidly. Hence the Cu<sup>II</sup>-L2 is a steady state where Cu cycles slowly between Cu<sup>II</sup> and Cu<sup>I</sup>, with the reduction as rate limiting step. Cu<sup>II</sup>-L2 is reduced faster under anaerobic conditions, again indicating that reoxidation by O<sub>2</sub> occurs under aerobic conditions. This reoxidation is slower in absence of O<sub>2</sub>, so that GSH is able to retrieve Cu<sup>I</sup> from L2. Concerning Cu<sup>II</sup>-L1, its reduction went to completion in absence of O<sub>2</sub>, which was not the case under aerobic conditions, again suggesting that under aerobic conditions some reoxidation occurred.

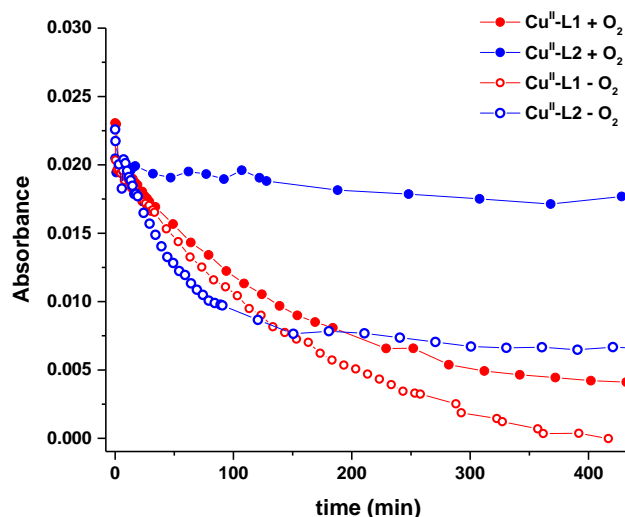


**Figure 8.** Absorbance of the d-d band of Cu<sup>II</sup>-L1 and Cu<sup>II</sup>-L2 in the presence and absence of oxygen upon time. Conditions: 220  $\mu$ M L, 200  $\mu$ M CuCl<sub>2</sub>, 2 mM GSH, 50 mM HEPES buffer pH 7.4. Experiments were carried out as triplicates and representative experiments are shown.

To have a good signal to noise ratio of the weak d-d bands, quite high Cu<sup>II</sup>-L concentrations were used. We repeated the same experiments at more biological relevant concentrations with 30  $\mu$ M Cu<sup>II</sup>-L and 3 mM GSH (Figure S26) and found similar behavior, Cu<sup>II</sup>-L2 was again much more stable aerobically than high Cu<sup>II</sup>-L1.

The UV-VIS spectroscopic results under aerobic conditions indicate that Cu<sup>II</sup>-L2 can redox-cycle in the presence of GSH, whereas Cu<sup>II</sup>-L1 loses its Cu to GSH. Hence, Cu<sup>II</sup>-L2 can catalyze the oxidation of GSH by O<sub>2</sub> without dissociation. Such reactions are of interest as they can deplete GSH and produce reactive oxygen species. Hence, we evaluated the reactivity by measuring the formation of the product GSSG (oxidized GSH) via HPLC and compared it to Cu<sup>II</sup>-Dp44mT (di-2-pyridylketone-4,4,-dimethyl-3-thiosemicarbazone), a complex able to deplete GSH in cancer cells and able to oxidize GSH in vitro although relatively slow.<sup>62</sup> Cu<sup>II</sup>-L1, Cu<sup>II</sup>-L2 and Cu<sup>II</sup> without ligand were able to catalyze GSH oxidation with very similar kinetics (Figure 9 and Figure S29). The reaction involving Cu<sup>II</sup>-L1, Cu<sup>II</sup>-L2 and Cu<sup>II</sup> was not terminated after 20 h and the initial turnover rate was calculated to be 4-5 cycles per hour. These initial rates were 2-3 times slower than the one measured for Cu-Dp44mT, which reached a plateau at about 12h.

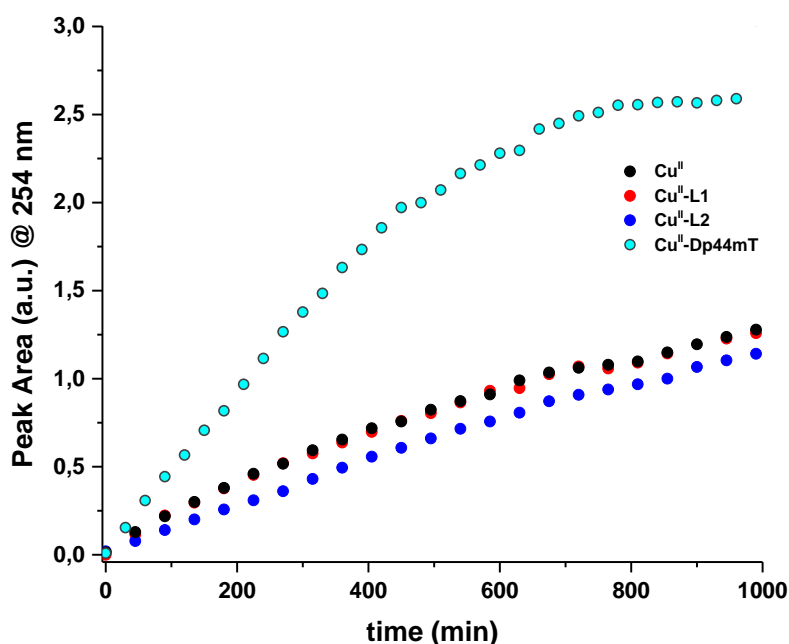


**Figure 9.** Monitoring of the GSH oxidation to GSSG by following the area of the GSSG peak at 254 nm by HPLC. Conditions: 30  $\mu$ M L, 27  $\mu$ M CuCl<sub>2</sub>, 3 mM GSH, 100 mM HEPES buffer pH 7.4, 2.2% DMSO for Dp44mT, gradient: 1-7% eluent B in 7 min.

Next the strong Cu<sup>I</sup>-(but weak Cu<sup>II</sup>) chelator bathocuproine disulfonate (BCS) was used to determine whether Cu<sup>I</sup> can be retrieved from the ligands L upon reduction by GSH (Figure 10). Indeed, BCS has been used to mimic the presence of strong Cu<sup>I</sup>-binding proteins in the cytosol of cells.<sup>63</sup> Cu<sup>I</sup>-BCS, but not BCS alone, is known to present an intense absorption band at 483 nm and a high affinity for Cu<sup>I</sup> (log  $\beta$  = 20.8).<sup>64</sup> Upon addition of 3 mM GSH to BCS in the presence of Cu<sup>II</sup> in the buffer the absorption band at 483 nm appeared very rapidly in less than a minute, due to reduction of Cu<sup>II</sup> to Cu<sup>I</sup> and its binding to BCS. When Cu<sup>II</sup> was coordinated to L1 or L2 and GSH added the Cu<sup>I</sup>-BCS<sub>2</sub> complex was formed with similar kinetics (Figure 10) and reached the same plateau as free Cu<sup>II</sup> after about approximately 50 min. The experiments of Cu<sup>II</sup>-L1 and Cu<sup>II</sup>-L2 were also repeated as a control in the absence of GSH, where no band at 483 nm rises. This suggests that upon reduction of Cu<sup>II</sup>-L to Cu<sup>I</sup>, Cu<sup>I</sup> is binding to BCS. The similar kinetics for the two complexes is in line with the similar reduction observed under anaerobic conditions (see above). Hence the difference between Cu<sup>II</sup>-L1 and Cu<sup>II</sup>-L2 is in the much faster reoxidation rate of Cu<sup>I</sup>-L2 by O<sub>2</sub> compared to Cu<sup>I</sup>-L1. Cu<sup>II</sup>-Dp44mT was also measured for comparison, and despite the fact that Cu<sup>II</sup>-Dp44mT is able to catalyze GSH oxidation (see above), which includes Cu<sup>I</sup> formation, BCS was not able to withdraw Cu<sup>I</sup> as no significant increase of the absorbance at 483 nm was observed over time. Furthermore, Cu<sup>II</sup>-L1 and Cu<sup>II</sup>-L2 were compared to the Cu-complexes measured by Xiao *et al.*<sup>63</sup>, *i.e.* the Cu<sup>II</sup>-ATSM (diacetylbis(4-methylthiosemicarbazone) and Cu<sup>II</sup>-GTSM (glyoxal-bis(N4-methyl-3-thiosemicarbazone), two bis(thiosemicarbazonato) complexes.

Confirming their findings, BCS was able to withdraw  $\text{Cu}^{\text{II}}$  from GTSM but not from ATSM in the presence of GSH (Figures S27 and S28).

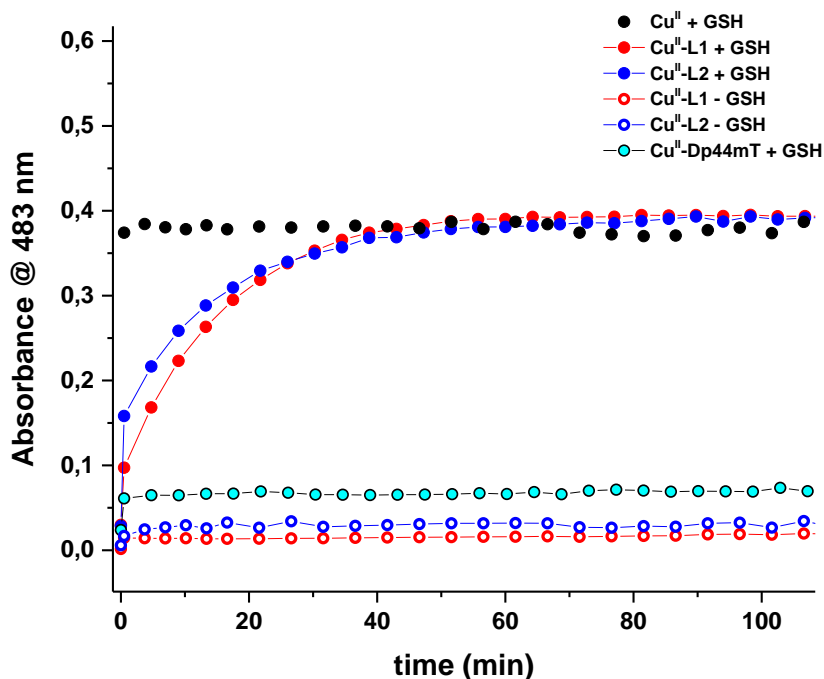


**Figure 10.** Following the absorbance of  $\text{Cu}^{\text{I}}(\text{BCS})_2$  at 483 nm over time. Conditions:  $30 \mu\text{M}$  L,  $27 \mu\text{M}$   $\text{Cu}^{\text{II}}$ ,  $67.5 \mu\text{M}$  BCS, (3 mM GSH), 100 mM HEPES pH 7.4, DMSO: 2.2% for Dp44mT.

## Conclusions

The synthesis and characterization of two  $\text{Cu}^{\text{II}}$  chelators L1 and L2, derivatives of the well-known peptide Xxx-Zzz-His/ATCUN motif, are reported.

L2 is a remarkable chelator as it was able to go beyond the affinity of all so far reported ATCUN motifs, reaching the level of the well-known chelator EDTA. But in contrast to EDTA, the selectivity towards  $\text{Cu}^{\text{II}}$  is very high, in particular over  $\text{Zn}^{\text{II}}$ , its most challenging competitor in biology. Even in the presence of HSA, that binds  $\text{Cu}^{\text{II}}$   $10^6$  times more tightly than  $\text{Zn}^{\text{II}}$ , L2 was able to bind  $\text{Cu}^{\text{II}}$  selectively. In contrast, EDTA binds  $\text{Cu}^{\text{II}}$  only about  $10^{2.5}$  times stronger than  $\text{Zn}^{\text{II}}$ .<sup>65</sup> The high affinity was obtained by replacing the N-terminal amine by a pyridine and by replacing one amide by an amine. Classically, the selectivity of the ATCUN for  $\text{Cu}^{\text{II}}$  over  $\text{Zn}^{\text{II}}$  is assigned to the capability of  $\text{Cu}^{\text{II}}$  to deprotonate amides for binding.<sup>23,66</sup> Recently, Jakusch *et al.*<sup>67</sup> (reported a  $10^{8.4}$  higher affinity of a related ligand (called DPMGA: N-(pyridin-2-ylmethyl)-2-((pyridin-2-ylmethyl)amino)acetamide) with the tetra-coordination of pyridine-amine-amide-pyridine (all 5-membered rings with  $\text{Cu}^{\text{II}}$ ). In line with their findings, our data confirm that one amidate coordination can still give a high selectivity for  $\text{Cu}^{\text{II}}$ , at least selective enough to bind  $\text{Cu}^{\text{II}}$  over  $\text{Zn}^{\text{II}}$  in the presence of HSA as it could occur in blood plasma. DPMGA showed a  $\log K_D$  of 14, i.e. about 2 logarithmic units lower than EDTA under standard conditions at pH 7.4. L2 had about the same affinity as EDTA at pH 7.4 in the present conditions. Despite the different conditions, the comparison with a reference compound such as EDTA suggests a stronger  $\text{Cu}^{\text{II}}$  affinity of L2 over DPMGA of about two log units. Structural differences that might explain this stronger affinity are the imidazole bound in a 6-membered ring compared to a pyridine with a 5-membered ring.

Not only the selectivity is kept for L2 compared to ATCUN, also the ability to redox silence Cu is still efficient. Indeed, L2 was able to stop the ascorbate oxidation catalyzed by  $\text{Cu}^{\text{II}}$  or  $\text{Cu}^{\text{II}}$  bound to  $\text{A}\beta_{1-16}$  in buffer as also reported for DPMGA<sup>67</sup>, again indicating that already one amidate can redox silence Cu

quite efficiently. Compared to L1, L2 is also kinetically faster in abstracting Cu from HSA and in redox silencing Cu bound to A $\beta$ <sub>1-16</sub>.

Another quite distinct feature of L2 compared to L1 or ATCUN is its resistance to 2 mM concentrations of GSH under aerobic conditions. GSH was not able to retrieve Cu via reduction and chelation from the complex Cu<sup>II</sup>-L2, whereas this retrieving was possible from Cu<sup>II</sup>-L1 as well as from other ATCUN motifs studied in the literature.<sup>60,61</sup>

Nevertheless, an intracellular environment is lower oxygenated than buffer and contains strong Cu<sup>I</sup>-binding and hence one can expect that both Cu<sup>II</sup>-L1 and -L2 would release Cu after slow reduction by GSH or other thiols to Cu<sup>I</sup>-binding proteins. This is supported by the retrieval of Cu<sup>I</sup> by the strong chelator BCS from Cu<sup>II</sup>-L in presence of GSH. This opens the possibility to use L2 as Cu-ionophore. Moreover, the redox reaction of Cu<sup>II</sup>-L2 with GSH is very slow, as it was with Asc, indicating that there is little danger of a high ROS production.

In summary, L2 has interesting Cu-binding properties for biological applications, in particular its fast and efficient redox-silencing of Cu, its selectivity, and its thermodynamic stability against HSA and its slow reactivity with mM GSH concentrations.

### Supporting Information

The supporting Information is available free of charge at Synthesis protocols of L1 and L2, NMR spectra, HR-ESI-MS, HPLC chromatograms, log *K* calculations, DFT data, additional UV-Vis-, CD- and EPR-spectra (PDF).

### Author information

Corresponding authors

Angélique Sour

Peter Faller

### Authors contributions

K.Z. performed synthesis of L1 and L2, Cu-binding studies, selectivity studies, reactivity measurements with AsC<sup>H</sup> and GSH, and contributed to analysis and writing. Be.V. performed measurements, analysis and writing of EPR part; C. P.-I. performed calculations, analysis and writing of DFT part; Bh.V. performed initial experiments and analysis of GSH oxidation and BCS test; P.F. supervised physico-chemical work and contributed to writing; A.S. synthesized GTSM, supervised synthetic work and contributed to writing.

### Acknowledgements

The French Ministry of Education and Research is acknowledged for a Ph.D. fellowship to Z.K.. C. P.-I. thanks Centro de Supercomputación de Galicia (CESGA) for providing access to supercomputing facilities. The authors thank Maiia Aleksandrova for preliminary results in the synthesis of L1 and L2, Paulina Gonzalez for providing ATSM, Michael Okafor for providing A $\beta$ <sub>1-16</sub> and Enrico Falcone for very useful discussions.

### Notes

The authors declare no conflict of interest.

### References

- (1) Davis, A. V; O'halloran, T. V. A Place for Thioether Chemistry in Cellular Copper Ion Recognition and Trafficking. *Nat. Chem. Biol.* **2008**, *4* (3), 148–151.

- (2) Morgan, M. T.; Nguyen, L. A. H.; Hancock, H. L.; Fahrni, C. J. Glutathione Limits Aquacopper(I) to Sub-Femtomolar Concentrations through Cooperative Assembly of a Tetranuclear Cluster. *J. Biol. Chem.* **2017**, *292* (52), 21558–21567.
- (3) Hill, W. E.; Reed, V. D. Oxidation of Thiols by Copper(II). *Phosphorus, Sulfur Silicon Relat. Elem.* **1994**, *90* (1–4), 147–154.
- (4) Linder, M. C. Copper Homeostasis in Mammals, with Emphasis on Secretion and Excretion. A Review. *Int. J. Mol. Sci.* **2020**, *21* (14), 4932.
- (5) Falcone, E.; Okafor, M.; Vitale, N.; Raibaut, L.; Sour, A.; Faller, P. Extracellular Cu<sup>2+</sup> Pools and Their Detection: From Current Knowledge to next-Generation Probes. *Coord. Chem. Rev.* **2021**, *433*, 213727.
- (6) Macomber, L.; Imlay, J. A. The Iron-Sulfur Clusters of Dehydratases Are Primary Intracellular Targets of Copper Toxicity. *Proc. Natl. Acad. Sci. U. S. A.* **2009**, *106* (20), 8344.
- (7) Lutsenko, S. Copper Trafficking to the Secretory Pathway. *Metallomics* **2016**, *8* (9), 840–852.
- (8) Zuily, L.; Lahrach, N.; Fassler, R.; Genest, O.; Faller, P.; Sénèque, O.; Denis, Y.; Castanié-Cornet, M.-P.; Genevaux, P.; Jakob, U.; Reichmann, D.; Giudici-Ortoni, M.-T.; Ilbert, M.; David, M.; Johnson, L. Copper Induces Protein Aggregation, a Toxic Process Compensated by Molecular Chaperones. *mBio* **2022**, *13* (2).
- (9) Tsvetkov, P.; Coy, S.; Petrova, B.; Dreishpoon, M.; Verma, A.; Abdusamad, M.; Rossen, J.; Joesch-Cohen, L.; Humeidi, R.; Spangler, R. D.; Eaton, J. K.; Frenkel, E.; Kocak, M.; Corsello, S. M.; Lutsenko, S.; Kanarek, N.; Santagata, S.; Golub, T. R. Copper Induces Cell Death by Targeting Lipoylated TCA Cycle Proteins. *Science (1979)* **2022**, *375* (6586), 1254–1261.
- (10) Wiebelhaus, N.; Zaengle-Barone, J. M.; Hwang, K. K.; Franz, K. J.; Fitzgerald, M. C. Protein Folding Stability Changes across the Proteome Reveal Targets of Cu Toxicity in E. Coli. *ACS Chem. Biol.* **2021**, *16* (1), 214.
- (11) Stewart, L. J.; Ong, C. L. Y.; Zhang, M. M.; Brouwer, S.; McIntyre, L.; Davies, M. R.; Walker, M. J.; McEwan, A. G.; Waldron, K. J.; Djoko, K. Y. Role of Glutathione in Buffering Excess Intracellular Copper in Streptococcus Pyogenes. *mBio* **2020**, *11* (6), 1–19.
- (12) Meyerstein, D. What Are the Oxidizing Intermediates in the Fenton and Fenton-like Reactions? A Perspective. *Antioxidants* **2022**, *11* (7).
- (13) Shen, J.; Griffiths, P. T.; Campbell, S. J.; Utinger, B.; Kalberer, M.; Paulson, S. E. Ascorbate Oxidation by Iron, Copper and Reactive Oxygen Species: Review, Model Development, and Derivation of Key Rate Constants. *Sci. Rep.* **2021**, *11* (1), 1–14.
- (14) Keown, W.; Gary, J. B.; Stack, T. D. P. High-Valent Copper in Biomimetic and Biological Oxidations. *J. Biol. Inorg. Chem.* **2017**, *22* (2–3), 289–305.
- (15) Elwell, C. E.; Gagnon, N. L.; Neisen, B. D.; Dhar, D.; Spaeth, A. D.; Yee, G. M.; Tolman, W. B. Copper-Oxygen Complexes Revisited: Structures, Spectroscopy, and Reactivity. *Chem. Rev.* **2017**, *117* (3), 2059–2107.
- (16) Jungwirth, U.; Kowol, C. R.; Keppler, B. K.; Hartinger, C. G.; Berger, W.; Heffeter, P. Anticancer Activity of Metal Complexes: Involvement of Redox Processes. *Antioxid. Redox Signaling* **2011**, *15* (4), 1085–1127.

- (17) Buettner, G. R.; Jurkiewicz, B. A. Catalytic Metals, Ascorbate and Free Radicals: Combinations to Avoid. *Radiat. Res.* **1996**, *145* (5), 532–541.
- (18) Huang, X.; Cuajungco, M. P.; Atwood, C. S.; Hartshorn, M. A.; Tyndall, J. D. A.; Hanson, G. R.; Stokes, K. C.; Leopold, M.; Multhaup, G.; Goldstein, L. E.; Scarpa, R. C.; Saunders, A. J.; Lim, J.; Moir, R. D.; Glabe, C.; Bowden, E. F.; Masters, C. L.; Fairlie, D. P.; Tanzi, R. E.; Bush, A. I. Cu(II) Potentiation of Alzheimer A $\beta$  Neurotoxicity. *J. Biol. Chem.* **1999**, *274* (52), 37111–37116.
- (19) Faller, P.; Hureau, C.; La Penna, G. Metal Ions and Intrinsically Disordered Proteins and Peptides: From Cu/Zn Amyloid- $\beta$  to General Principles. *Acc. Chem. Res.* **2014**, *47* (8), 2252–2259.
- (20) Atrián-Blasco, E.; Gonzalez, P.; Santoro, A.; Alies, B.; Faller, P.; Hureau, C. Cu and Zn Coordination to Amyloid Peptides: From Fascinating Chemistry to Debated Pathological Relevance. *Coord. Chem. Rev.* **2018**, *375*, 38.
- (21) Smith, D. G.; Cappai, R.; Barnham, K. J. The Redox Chemistry of the Alzheimer's Disease Amyloid  $\beta$  Peptide. *Biochim. Biophys. Acta* **2007**, *1768* (8), 1976–1990.
- (22) Harford, C.; Sarkar, B. Amino Terminal Cu(II)- and Ni(II)-Binding (ATCUN) Motif of Proteins and Peptides: Metal Binding, DNA Cleavage, and Other Properties. *Acc. Chem. Res.* **1997**, *30* (3), 123–130.
- (23) Gonzalez, P.; Bossak, K.; Stefaniak, E.; Hureau, C.; Raibaut, L.; Bal, W.; Faller, P. N-Terminal Cu Binding Motifs Xxx-Zzz-His (ATCUN) and Xxx-His and Their Derivatives: Chemistry, Biology and Medicinal Applications. *Chem. Eur. J.* **2018**, *24* (32), 8029.
- (24) Maiti, B. K.; Govil, N.; Kundu, T.; Moura, J. J. G. Designed Metal-ATCUN Derivatives: Redox- and Non-Redox-Based Applications Relevant for Chemistry, Biology, and Medicine. *iScience* **2020**, *23* (12).
- (25) Kotuniak, R.; Bal, W. Kinetics of Cu(II) Complexation by ATCUN/NTS and Related Peptides: A Gold Mine of Novel Ideas for Copper Biology. *Dalton Trans.* **2021**, *51* (1), 14–26.
- (26) Santoro, A.; Walke, G.; Vilenko, B.; Kulkarni, P. P.; Raibaut, L.; Faller, P. Low Catalytic Activity of the Cu(II)-Binding Motif (Xxx-Zzz-His; ATCUN) in Reactive Oxygen Species Production and Inhibition by the Cu(I)-Chelator BCS. *Chem. Commun.* **2018**, *54* (84), 11945–11948.
- (27) Jin, Y.; Lewis, M. A.; Gokhale, N. H.; Long, E. C.; Cowan, J. A. Influence of Stereochemistry and Redox Potentials on the Single- and Double-Strand DNA Cleavage Efficiency of Cu(II)- and Ni(II)-Lys-Gly-His- Derived ATCUN Metallopeptides. *J. Am. Chem. Soc.* **2007**, *129* (26), 8353–8361.
- (28) Neupane, K. P.; Aldous, A. R.; Kritzer, J. A. Metal-Binding and Redox Properties of Substituted Linear and Cyclic ATCUN Motifs. *J. Inorg. Biochem.* **2014**, *139*, 65–76.
- (29) Wiloch, M. Z.; Ufnalska, I.; Bonna, A.; Bal, W.; Wróblewski, W.; Wawrzyniak, U. E. Copper(II) Complexes with ATCUN Peptide Analogues: Studies on Redox Activity in Different Solutions. *J. Electrochem. Soc.* **2017**, *164* (7), G77–G81.
- (30) Wong, L. F.; Cooper, J. C.; Margerum, D. W. Kinetics of Copper(II)--Glycylglycyl-L-Histidine Reactions. Acid Decomposition and Proton-Assisted Nucleophilic Displacement by Triethylenetetramine. *J. Am. Chem. Soc.* **1976**, *98* (23), 7268–7274.

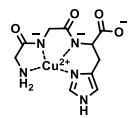
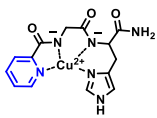
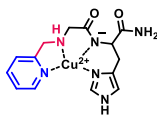


- (31) Jin, Y.; Cowan, J. A. DNA Cleavage by Copper-ATCUN Complexes. Factors Influencing Cleavage Mechanism and Linearization of DsDNA. *J. Am. Chem. Soc.* **2005**, *127* (23), 8408–8415.
- (32) Kotuniak, R.; Strampraad, M. J. F.; Bossak-Ahmad, K.; Wawrzyniak, U. E.; Ufnalska, I.; Hagedoorn, P. L.; Bal, W. Key Intermediate Species Reveal the Copper(II)-Exchange Pathway in Biorelevant ATCUN/NTS Complexes. *Angew. Chem., Int. Ed. Engl.* **2020**, *59* (28), 11234.
- (33) Portelinha, J.; Duay, S. S.; Yu, S. I.; Heilemann, K.; Libardo, M. D. J.; Juliano, S. A.; Klassen, J. L.; Angeles-Boza, A. M. Antimicrobial Peptides and Copper(II) Ions: Novel Therapeutic Opportunities. *Chem. Rev.* **2021**, *121* (4), 2648–2712.
- (34) Vázquez, G.; Caballero, A. B.; Kokinda, J.; Hijano, A.; Sabaté, R.; Gamez, P. Copper, Dityrosine Cross-Links and Amyloid- $\beta$  Aggregation. *J. Biol. Inorg. Chem.* **2019**, *24* (8), 1217–1229.
- (35) Lefèvre, M.; Malikidogo, K. P.; Esmieu, C.; Hureau, C. Sequence–Activity Relationship of ATCUN Peptides in the Context of Alzheimer’s Disease. *Molecules* **2022**, *27* (22), 7903.
- (36) Heinrich, J.; Bossak-Ahmad, K.; Riisom, M.; Haeri, H. H.; Steel, T. R.; Hergl, V.; Langhans, A.; Schattschneider, C.; Barrera, J.; Jamieson, S. M. F.; Stein, M.; Hinderberger, D.; Hartinger, C. G.; Bal, W.; Kulak, N. Incorporation of  $\beta$ -Alanine in Cu(II) ATCUN Peptide Complexes Increases ROS Levels, DNA Cleavage and Antiproliferative Activity. *Chem.-Eur. J.* **2021**, *27* (72), 18093–18102.
- (37) Perrone, L.; Mothes, E.; Vignes, M.; Mockel, A.; Figueroa, C.; Miquel, M. C.; Maddelein, M. L.; Faller, P. Copper Transfer from Cu-Abeta to Human Serum Albumin Inhibits Aggregation, Radical Production and Reduces Abeta Toxicity. *ChemBioChem* **2010**, *11* (1), 110–118.
- (38) Hu, X.; Zhang, Q.; Wang, W.; Yuan, Z.; Zhu, X.; Chen, B.; Chen, X. Tripeptide GGH as the Inhibitor of Copper-Amyloid- $\beta$ -Mediated Redox Reaction and Toxicity. *ACS Chem. Neurosci.* **2016**, *7* (9), 1255–1263.
- (39) Caballero, A. B.; Terol-Ordaz, L.; Espargaró, A.; Vázquez, G.; Nicolás, E.; Sabaté, R.; Gamez, P. Histidine-Rich Oligopeptides To Lessen Copper-Mediated Amyloid- $\beta$  Toxicity. *Chem. Eur. J.* **2016**, *22* (21), 7268–7280.
- (40) Folk, D. S.; Franz, K. J. A Prochelator Activated by  $\beta$ -Secretase Inhibits A $\beta$  Aggregation and Suppresses Copper-Induced Reactive Oxygen Species Formation. *J. Am. Chem. Soc.* **2010**, *132* (14), 4994–4995.
- (41) Mital, M.; Sęk, J. P.; Ziora, Z. M. Metal–Peptide Complexes to Study Neurodegenerative Diseases. *Methods in Molecular Biology* **2020**, *2103*, 323–336.
- (42) Mital, M.; Wezynfeld, N. E.; Frączyk, T.; Wiloch, M. Z.; Wawrzyniak, U. E.; Bonna, A.; Tumpach, C.; Barnham, K. J.; Haigh, C. L.; Bal, W.; Drew, S. C. A Functional Role for A $\beta$  in Metal Homeostasis? N-Truncation and High-Affinity Copper Binding. *Angew. Chem., Int. Ed.* **2015**, *54* (36), 10460–10464.
- (43) Sigel, H.; Martin, R. B. Coordinating Properties of the Amide Bond. Stability and Structure of Metal Ion Complexes of Peptides and Related Ligands. *Chem. Rev.* **1982**, *82* (4), 385–426.
- (44) Camerman, N.; Camerman, A.; Sarkar, B. Molecular Design to Mimic the Copper(II) Transport Site of Human Albumin. The Crystal and Molecular Structure of Copper(II) – Glycylglycyl-L-Histidine-N-Methyl Amide Monoquo Complex. *Can. J. Chem.* **1976**, *54* (8), 1309–1316.

- (45) Kossmann, S.; Kirchner, B.; Neese, F.; Kossmann, S.; Kirchner, B. Performance of Modern Density Functional Theory for the Prediction of Hyperfine Structure: Meta-GGA and Double Hybrid Functionals. *Mol. Phys.* **2008**, *105* (15–16), 2049–2071.
- (46) AlHaddad, N.; Lelong, E.; Suh, J. M.; Cordier, M.; Lim, M. H.; Royal, G.; Platas-Iglesias, C.; Bernard, H.; Tripier, R. Copper(II) and Zinc(II) Complexation with N-Ethylene Hydroxycyclams and Consequences on the Macrocyclic Backbone Configuration. *Dalton Trans.* **2022**, *51* (22), 8640–8656.
- (47) Drosou, M.; Mitsopoulou, C. A.; Orio, M.; Pantazis, D. A. EPR Spectroscopy of Cu(II) Complexes: Prediction of g-Tensors Using Double-Hybrid Density Functional Theory. *Magnetochemistry* **2022**, *8* (4), 36.
- (48) Kirsipuu, T.; Zadorožnaja, A.; Smirnova, J.; Friedemann, M.; Plitz, T.; Tõugu, V.; Palumaa, P. Copper(II)-Binding Equilibria in Human Blood. *Sci. Rep.* **2020**, *10* (1), 1–11.
- (49) Xiao, Z.; Wedd, A. G. The Challenges of Determining Metal-Protein Affinities. *Nat. Prod. Rep.* **2010**, *27* (5), 768–789.
- (50) Harris, W. R.; Carrano, C. J.; Raymond, K. N. Spectrophotometric Determination of the Proton-Dependent Stability Constant of Ferric Enterobactin. *J. Am. Chem. Soc.* **1979**, *101* (8), 2213–2214.
- (51) Frączyk, T. Phosphorylation Impacts Cu(II) Binding by ATCUN Motifs. *Inorg. Chem.* **2021**, *60* (12), 8447–8450.
- (52) Bossak-Ahmad, K.; Frączyk, T.; Bal, W.; Drew, S. C. The Sub-Picomolar Cu<sup>2+</sup> Dissociation Constant of Human Serum Albumin. *ChemBioChem* **2020**, *21* (3), 331–334.
- (53) Coverdale, J. P. C.; Khazaipoul, S.; Arya, S.; Stewart, A. J.; Blindauer, C. A. Crosstalk between Zinc and Free Fatty Acids in Plasma. *Biochim. Biophys. Acta Mol. Cell. Biol. Lipids* **2019**, *1864* (4), 532–542.
- (54) Bal, W.; Sokołowska, M.; Kurowska, E.; Faller, P. Binding of Transition Metal Ions to Albumin: Sites, Affinities and Rates. *Biochim. Biophys. Acta* **2013**, *1830* (12), 5444–5455.
- (55) Bal, W.; Christodoulou, J.; Sadler, P. J.; Tucker, A. Multi-Metal Binding Site of Serum Albumin. *J. Inorg. Biochem.* **1998**, *70* (1), 33–39.
- (56) Alies, B.; Sasaki, I.; Proux, O.; Sayen, S.; Guillon, E.; Faller, P.; Hureau, C. Zn Impacts Cu Coordination to Amyloid- $\beta$ , the Alzheimer's Peptide, but Not the ROS Production and the Associated Cell Toxicity. *Chem. Commun.* **2013**, *49* (12), 1214.
- (57) Pedersen, J. T.; Chen, S. W.; Borg, C. B.; Ness, S.; Bahl, J. M.; Heegaard, N. H. H.; Dobson, C. M.; Hemmingsen, L.; Cremades, N.; Teilum, K. Amyloid- $\beta$  and  $\alpha$ -Synuclein Decrease the Level of Metal-Catalyzed Reactive Oxygen Species by Radical Scavenging and Redox Silencing. *J. Am. Chem. Soc.* **2016**, *138* (12), 3966–3969.
- (58) Guilloreau, L.; Combalbert, S.; Sournia-Saquet, M.; Mazarguil, H.; Faller, P. Redox Chemistry of Copper–Amyloid- $\beta$ : The Generation of Hydroxyl Radical in the Presence of Ascorbate Is Linked to Redox-Potentials and Aggregation State. *ChemBioChem* **2007**, *8* (11), 1317–1325.
- (59) Hakuna, L.; Doughan, B.; Escobedo, J. O.; Strongin, R. M. A Simple Assay for Glutathione in Whole Blood. *Analyst* **2015**, *140* (10), 3339–3342.

- (60) Santoro, A.; Ewa Wezynfeld, N.; Vařák, M.; Bal, W.; Faller, P. Cysteine and Glutathione Trigger the Cu-Zn Swap between Cu(II)-Amyloid- $\beta$  4-16 Peptide and Zn 7-Metallothionein-3. *Chem. Commun.* **2017**, 53 (85), 11634–11637.
- (61) Stefaniak, E.; Płonka, D.; Szczerba, P.; Wezynfeld, N. E.; Bal, W. Copper Transporters? Glutathione Reactivity of Products of Cu- $\text{A}\beta$  Digestion by Neprilysin. *Inorg. Chem.* **2020**, 59 (7), 4186–4190.
- (62) Falcone, E.; Ritacca, A. G.; Hager, S.; Schueffl, H.; Vileno, B.; El Khoury, Y.; Hellwig, P.; Kowol, C. R.; Heffeter, P.; Sicilia, E.; Faller, P. Copper-Catalyzed Glutathione Oxidation Is Accelerated by the Anticancer Thiosemicarbazone Dp44mT and Further Boosted at Lower PH. *J. Am. Chem. Soc.* **2022**, 144 (32), 14758–14768.
- (63) Xiao, Z.; Donnelly, P. S.; Zimmermann, M.; Wedd, A. G. Transfer of Copper between Bis(Thiosemicarbazone) Ligands and Intracellular Copper-Binding Proteins. Insights into Mechanisms of Copper Uptake and Hypoxia Selectivity. *Inorg. Chem.* **2008**, 47 (10), 4338–4347.
- (64) Bagchi, P.; Morgan, M. T.; Bacsa, J.; Fahrni, C. J. Robust Affinity Standards for Cu(I) Biochemistry. *J. Am. Chem. Soc.* **2013**, 135 (49), 18549.
- (65) Ogino, H.; The Stability Constants of Ethylenediaminetetraacetato, Trimethylenediaminetetraacetato and Propylenediaminetetraacetato Complexes of Some Divalent Metal Ions. *Bull. Chem. Soc. Jpn.* **2006**, 38 (5), 771–777.
- (66) Sívágó, I.; Kállay, C.; Várnagy, K. Peptides as Complexing Agents: Factors Influencing the Structure and Thermodynamic Stability of Peptide Complexes. *Coord. Chem. Rev.* **2012**, 256 (19–20), 2225–2233.
- (67) Jakusch, T.; Hassoon, A. A.; Kiss, T. Characterization of Copper(II) Specific Pyridine Containing Ligands: Potential Metallophores for Alzheimer's Disease Therapy. *J. Inorg. Biochem.* **2022**, 228, 111692.

## TOC

			
	Cu <sup>II</sup> -GGH	Cu <sup>II</sup> -L1	Cu <sup>II</sup> -L2
Affinity $\log K_{\text{pH } 7.4}^{\text{app}}$	12.4	13.6	16.0
Selectivity Cu <sup>II</sup> > Zn <sup>II</sup>	<input checked="" type="checkbox"/>	<input checked="" type="checkbox"/>	<input checked="" type="checkbox"/>
Redox silencing	<input checked="" type="checkbox"/>	<input checked="" type="checkbox"/>	<input checked="" type="checkbox"/>

## Synopsis

Two new Cu<sup>II</sup>-ligand complexes (Cu<sup>II</sup>-L1 and Cu<sup>II</sup>-L2) inspired by the well-known N-terminal peptidic motif Xxx-Zzz-His, also called ATCUN motif, are reported. The replacement of the amine and amidate by a pyridine and amine respectively, increased substantially the Cu<sup>II</sup>-affinity of L2 up to the range of

EDTA. At the same time, Cu<sup>II</sup>-L2 also kept several properties of the parent ATCUN motif, in particular the high selectivity for Cu<sup>II</sup> and the redox silencing of Cu<sup>II</sup> in this complex.